www.nature.com/cmi

ARTICLE

Naturally occurring spike mutations influence the infectivity and immunogenicity of SARS-CoV-2

Qiaoli Peng[1,2,3,7], Runhong Zhou[1,3,4,7], Na Liu[5,7], Hui Wang[2,7], Haoran Xu[1,3], Meiqing Zhao[1,3], Dawei Yang[1,3], Ka-Kit Au[1,3], Haode Huang[1,3], Li Liu[1,3,4] and Zhiwei Chen[1,3,4,5,6]✉

Mutations in SARS-CoV-2 variants of concern (VOCs) have enhanced transmissibility and immune evasion with respect to current vaccines and neutralizing antibodies (NAbs). How naturally occurring spike mutations affect the infectivity and antigenicity of VOCs remains to be investigated. The entry efficiency of individual spike mutations was determined in vitro using pseudotyped viruses. BALB/c mice were immunized with 2-dose DNA vaccines encoding B.1.1.7, B.1.351, B.1.1.529 and their single mutations. Cellular and humoral immune responses were then compared to determine the impact of individual mutations on immunogenicity. In the B.1.1.7 lineage, Del69–70 and Del 144 in NTD, A570D and P681H in SD1 and S982A and D1118H in S2 significantly increased viral entry, whereas T716I resulted in a decrease. In the B.1.351 lineage, L18F and Del 242–244 in the NTD, K417N in the RBD and A701V in S2 also increased viral entry. S982A weakened the generation of binding antibodies. All sera showed reduced cross-neutralization activity against B.1.351, B.1.617.2 (Delta) and B.1.1.529 (Omicron BA.1). S982A, L18F, and Del 242–244 hindered the induction of cross-NAbs, whereas Del 69–70, Del144, R246I, and K417N showed the opposite effects. B.1.351 elicited adequate broad cross-NAbs against both B.1.351 and B.1.617.2. All immunogens tested, however, showed low neutralization against circulating B.1.1.529. In addition, T-cell responses were unlikely affected by mutations tested in the spike. We conclude that individual spike mutations influence viral infectivity and vaccine immunogenicity. Designing VOC-targeted vaccines is likely necessary to overcome immune evasion from current vaccines and neutralizing antibodies.

Keywords: SARS-CoV-2; Variants of Concern; Single mutation; neutralizing antibody; T cell responses; vaccine immunogenicity

Cellular & Molecular Immunology (2022) 19:1302–1310; https://doi.org/10.1038/s41423-022-00924-8

INTRODUCTION

Severe acute respiratory syndrome coronavirus 2 (SARS-CoV-2) is the causative agent of the COVID-19 pandemic, which has resulted in more than 5.92 million deaths globally (25 Feb, 2022). Multiple effective vaccines based on wild-type (WT) Wuhan-Hu-1 have been available since late 2020, and most of them showed extraordinary efficacy in providing protection against symptomatic infection as well as reducing hospitalizations, severity and mortality in their respective clinical trials [1–5] and subsequent real-world situations [6–8].

However, with the emergence of SARS-CoV-2 variants of concern (VOCs), mutations and deletions in the spike protein have altered the fitness to the host and susceptibility to population immunity, thus posing great challenges to the control of the ongoing pandemic. The cellular entry of SARS-CoV-2 is primarily mediated by binding of the receptor binding domain (RBD) to the host receptor angiotensin-converting enzyme 2 (ACE2). Any mutations in the RBD or spike protein that change the conformational structure of the RBD may impact viral transmissibility. In line with this, the D614G substitution facilitates ACE2 receptor binding by modifying the RBD position to an open state [9, 10]. Several mutations in RBD, such as N501Y [11], L452R [12], N439K [13], Y453F [14], and S477N [14], were also reported to increase the affinity of ACE2 binding. In addition, deletions at residues 69–70 of the NTD are related to increased virus replication in the upper respiratory tract [15]. More importantly, several mutations in the RBD (E484K, L452R, K417T) and NTD (L18F, Del 144 and Del 242–244) have conferred substantial resistance to infection- or vaccine-induced immunity and to neutralizing antibodies (NAbs) [16, 17]. Neutralizing antibody effectiveness against B.1.351 (Beta), P1 (Gamma), B.1.617.2 (Delta) and B.1.1.529 (Omicron BA.1) lineages was reported to drop dramatically 3- to 40-fold compared to the WT [17–21]. Breakthrough infections by B.1.617.2 and B.1.1.529 lineages have led to

[1]AIDS Institute, Li Ka Shing Faculty of Medicine, The University of Hong Kong, Hong Kong Special Administrative Region, PR China. [2]National Clinical Research Center for Infectious Diseases, HKU AIDS Institute Shenzhen Research Laboratory, The Third People's Hospital of Shenzhen and The Second Affiliated Hospital of Southern University of Science and Technology, Shenzhen, Guangdong, PR China. [3]Department of Microbiology, Li Ka Shing Faculty of Medicine, The University of Hong Kong, Hong Kong Special Administrative Region, PR China. [4]Centre for Virology, Vaccinology and Therapeutics Limited, The University of Hong Kong, Hong Kong Special Administrative Region, PR China. [5]HKU AIDS Institute Joint Laboratory, Department of Clinical Microbiology and Infection Control, The University of Hong Kong-Shenzhen Hospital, Shenzhen, Guangdong, PR China. [6]State Key Laboratory of Emerging Infectious Disease, The University of Hong Kong, Hong Kong Special Administrative Region, PR China. [7]These authors contributed equally: Qiaoli Peng, Runhong Zhou, Na Liu, Hui Wang. ✉email: zchenai@hku.hk

Received: 27 April 2022 Accepted: 28 August 2022
Published online: 12 October 2022

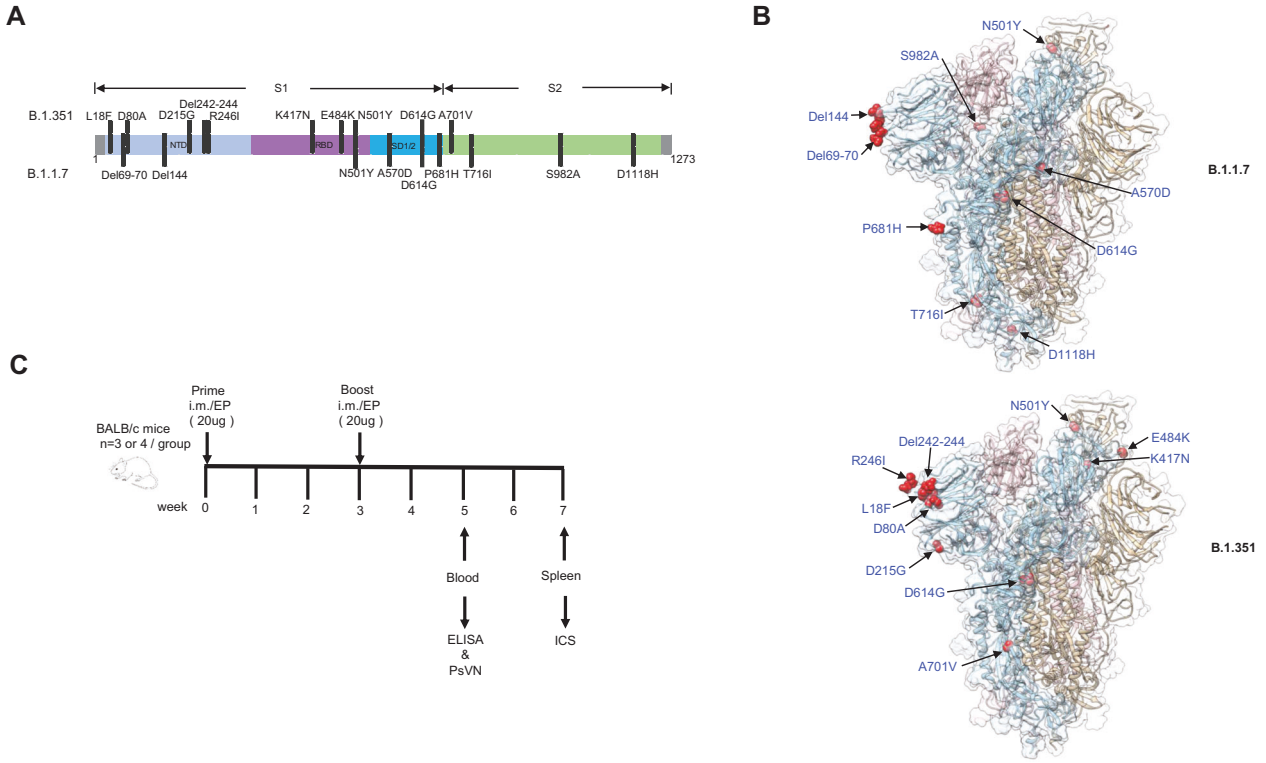

Fig. 1 Schematic of the study strategy. **A** Mutations in the spike of B.1.1.7 (Alpha) and B.1.351 (Beta) involved in this study. **B** The position display of substitutions or deletions in B.1.1.7 (Alpha) and B.1.351 (Beta) spike structure. **C** Immunization strategy and experimental schedule. Mice were primed and boosted on weeks 0 and 3 with DNA immunogens, including all the single mutation-containing variants and the D614G, B.1.1.7, and B.1.351 lineages

globally spread even in countries with the highest mRNA vaccination coverage [22–25]. These viral variants severely challenge the efficacy of WT-based vaccines. However, the immune response elicited among B.1.351-infected patients indicated robust cross-reactive NAb responses against both WT and new variants, indicating that the impact of spike mutations on immunogenicity should be considered for the optimization of next-generation vaccines [26]. In this regard, comprehensive mapping of naturally occurring spike mutations and their effects on viral infectivity and immunogenicity is of great importance. In this study, BALB/c mice were immunized with a 2-dose DNA vaccine encoding B.1.1.7, B.1.351 and B.1.1.529 lineages as well as their distinct single mutations. We determined the impact of individual mutations on viral entry and immune cross-reactivity, including both humoral and cellular responses.

METHODS

Variant spike mutation-containing DNA vaccine plasmid construction

Plasmids encoding SARS-CoV-2 variants (D614G, B.1.1.7 and B.1.351) as well as all the single mutation variants of the B.1.1.7 and B.1.351 lineages (D614G/L18F, D614G/Del69–70, D614G/D80A, D614G/Del144, D614G/D215G, D614G/Del 242–244, D614G/R246I, D614G/K417N, D614G/E484K, D614G/N501Y, D614G/A570D, D614G/P681H, D614G/A701V, D614G/T716I, D614G/S982A, D614G/D1118H) (Fig. 1A, B and Supplementary Table 1) were kindly provided by Professor David. Ho from Columbia University. Other plasmids encoding single mutation variants of the RBD of B.1.1.529 (D614G/S375F, D614G/S373P, D614G/G339D, D614G/N440K, D614G/G446S, D614G/T478K, D614G/S477N, D614G/E484A, D614G/Q493R, D614G/Q498R, D614G/Y505H, D614G/G496S, D614G/L452R, D614G/S371L) were produced by our laboratory (Supplementary Tables 2, 3). Briefly, all these plasmids were generated by a QuikChange II XL site-directed mutagenesis kit (Agilent, Cat# 200522) based on the original pCMV3-SARS-CoV-2-spike plasmid [16]. All plasmids were confirmed by sequence analysis. Each plasmid was purified with an Endofree Plasmid Maxi Kit (Qiagen, Cat# 12362), and the concentration was measured using a Nanodrop 8000 based on the average of four individual tests.

Schematic of mouse immunization strategy

All animal experiments were carried out with approval from the Committee on the Use of Live Animals in Teaching and Research of the University of Hong Kong (HKU). For vaccine immunization, 6-week-old male BALB/c mice were used. DNA vaccine plasmids (20 μg) were diluted in 100 μl of 1× phosphate buffered saline (PBS). The mice were inoculated via intramuscular/electroporation (i.m./EP) at week 0 and 3. Peripheral blood was taken at week 5. All mice were sacrificed to obtain the spleen at week 7 (Fig. 1C). The voltage of EP was preset to 60 V in the TERESA DNA Delivery Device (Shanghai Teresa Healthcare Sci-Tech Co., Ltd).

Enzyme-linked immunosorbent assay (ELISA)

ELISA was used to determine IgG binding to the RBD and the full spike protein as we previously described [27]. The area under the curve (AUC) of each sample, representing the total peak area based on ELISA OD values as previously described [28], was plotted using GraphPad Prism v8, and the baseline with the defined endpoint was set as the average of negative control wells + 10 standard deviations. The limit of quantification (LOQ) was established based on the geometric mean of PBS-vaccinated mice without a prior SARS-CoV-2 infection history.

Pseudotyped viral neutralization assay

The spike-expressing plasmids encoding the wild-type, the D614G, B.1.1.7, B.1.351, P1, B.1.617.2, B.1.1.529 variants and B.1.1.7 and B.1.351 bearing single site mutants were used to generate pseudoviruses. P1 was purchased from InvivoGen, while the others were made by us or collaborators. Briefly, SARS-CoV-2 pseudoviruses were generated by cotransfection of 293T cells with a pair of plasmids, the spike-expressing plasmid for WT or VOCs and the pNL4–3Luc_Env_Vpr plasmid in a human immunodeficiency virus type 1 backbone [29, 30]. At 48 h post-transfection, virus-containing supernatant was collected, quantified by determining the TCID50 value in the HEK293T-hACE2 cell line, and frozen

at −150 °C. The pseudotyped neutralization assay of vaccinated samples was performed as previously described [21, 29, 30]. Serially diluted and heat-inactivated plasma samples were incubated with 200 TCID50 of pseudovirus at 37 °C for 1 h. The plasma-virus mixtures were then added to preseeded HEK 293T-hACE2 cells. After 48 h, infected cells were lysed, and luciferase activity was measured using the Luciferase Assay System Kit (Promega) in a Victor3–1420 Multilabel Counter (PerkinElmer). The 50% inhibitory concentrations (IC_{50}) of each specimen were calculated using nonlinear regression in GraphPad Prism v8 to reflect anti-SARS-CoV-2 antibody potency. Samples that failed to reach 50% inhibition at the lowest serum dilution of 1:20 were considered to be nonneutralizing, and the IC_{50} values were set to 10.

Pseudovirus entry assay

The pseudovirus was generated as mentioned above. After pseudovirus-containing culture supernatants were harvested, p24 was measured (HIV-1 p24; Sinobiological, Cat # 11695) by ELISA. HEK293T-ACE2 cells (10,000 cells per well in 100 µl) were plated in 96-well plates at 37 °C overnight. On the following day, pseudotyped virus containing 2 ng of p24 was added to the cells. After 48 h, infected cells were lysed, and luciferase activity was measured using the Luciferase Assay System kit (Promega) in a Victor3–1420 Multilabel Counter (PerkinElmer). Fold changes in relative luminescence units (RLUs) relative to the D614G variant were calculated. All mutants were tested in quadruplicate.

Peptide pools

We purchased a peptide pool of 15 amino acids (aa) overlapping by 11 aa spanning the full length of the SARS-CoV-2 spike (a total of 316 peptides) as well as single spike mutation-containing peptides in the B.1.1.7, B.1.351 and B.1.1.529 RBD from GeneScipt. The detailed composition of the peptide pools used for T-cell stimulation is provided in Supplementary Table 4.

Intracellular cytokine staining

To measure the antigen-specific T-cell response, spleen cells were isolated and stimulated with 2 µg/mL of the indicated COVID-19 antigen peptide pools spanning the ancestral SARS-CoV-2 spike or different mutation-containing peptide pools (Supplementary Table 4). Cells were incubated at 37 °C overnight, and BFA (Sigma) was added at 2 h post-incubation, as previously described [27]. PMA and ionomycin were included as positive controls. Stimulation with medium alone was used as a negative control. After overnight incubation, the cells were washed with staining buffer (PBS containing 2% FBS) and stained with mAbs against surface markers (Zombie Aqua, Percp-Cy5.5 anti-CD4, FITC anti-CD8) (Biolegend). For intracellular staining, cells were fixed and permeabilized with BD Cytofix/Cytoperm (BD Biosciences) prior to staining with mAbs against cytokines (APC anti-IFN-γ) (Biolegend) with Perm/Wash buffer (BD Biosciences). After gating on $CD4^+$ T and $CD8^+$ T cells, intracellular IFN-γ was calculated (Fig. S1). All percentages of antigen-specific $CD4^+$ and $CD8^+$ T cells were reported as background subtracted data from the same sample stimulated with negative control (medium only). The LOQ for antigen-specific $CD4^+$ and $CD8^+$ T-cell responses was calculated using a twofold median value of all negative controls. Samples with responses >LOQ and a stimulation index of >2 for $CD4^+$ and $CD8^+$ T cells were considered positive responders.

Binding affinity determination with spike-expressing transfected 293T cells by flow cytometry

First, 293T cells were transfected with variants bearing spike-expressing plasmids. Forty-eight hours later, the cells were harvested, washed and divided into aliquots. 293T cells alone were used as a negative control. The specified mutant-immunized inactivated sera were added to the same mutant-containing spike-transfected 293T cells at a dilution of 1:100 and incubated at 4 °C for 30 min. After washing with FACS buffer 2 times, the cells were incubated with Alexa Fluor 568 goat anti-mouse IgG secondary antibody (Life Technologies, Cat# A11004) and Zombie Aqua at 4 °C for 30 min. The percentage of positive cells relative to the negative control represented those with the ability to bind to its specific antigen.

Spike protein expression in vitro determined by western blotting

First, 293T cells were transfected with 2 µg of plasmid. Forty-eight hours later, the cells were harvested and lysed in RIPA buffer. The supernatants were collected, and the protein concentration was quantified by a Pierce™ BCA protein assay (Thermo Scientific, Cat# 23227). Then, 20 µg of total protein was mixed with sample loading buffer with 10% β-mercaptoethanol. Samples were subjected to SDS–PAGE at 120 V and transferred at 0.15 A to PVDF membranes. Membranes were probed with rabbit anti-SARS-CoV S1 subunit (diluted 1/1000; Sino Biological, Cat# 40150-T62) and mouse anti-β actin (diluted 1/6000; Abcam, Cat #6276). Near-infrared secondary antibodies, namely, IRDye 680RD goat anti-rabbit (diluted 1/10,000; Abcam, Cat# 216777) and IRDye 800CW goat anti-mouse (diluted 1/10,000; Abcam, Cat#216772), were subsequently used. Western blots were scanned by a Sapphire Biomolecular Imager with Sapphire Capture Software V1.7.0319.0. (Thermo Scientific Biosystems). ImageJ was used to calculate the fold change in spike expression relative to the housekeeping gene β-actin.

Statistical analysis

Flow cytometric data were analyzed using FlowJo 10.6.0. Statistical analysis was performed using GraphPad Prism v8. Unpaired Student's *t* test was used to compare between-group continuous values. The statistical method of aggregation used for the analysis of binding and neutralizing antibody titers (NAbTs) is the mean with the corresponding 95% confidence intervals (95% CI). The statistical details are depicted in the respective legends. $P < 0.05$ was considered statistically significant.

RESULTS

Naturally occurring spike mutations affect viral entry of SARS-CoV-2 variants

To address the effect of single naturally occurring spike mutations on viral entry, different SARS-CoV-2 variants pseudotyped with individual mutations in the B.1.1.7 lineage (Del 69–70, Del 144, N501Y, A570D, P681H, T716I, S982A and D1118H) and the B.1.351 lineage (L18F, D80A, D215G, Del242–244, R246I, K417N, E484K, N501Y, A701V) were generated for comparison. After viral quantification by measuring HIV-1 p24 protein, the same amount of each pseudovirus was used to infect HEK293T-ACE2 cells. Several variants in the B.1.1.7 lineage infected HEK293T-ACE2 cells with approximately 1.95–46.3-fold higher activity than that of the D614G control: 2.95-fold (95% CI 2.66–3.24, $P < 0.0001$) for Del 69–70, 1.95-fold (95% CI 1.61–2.29, $P < 0.0001$) for Del 144, 3.33-fold (95% CI 3.18–3.47, $P < 0.0001$) for A570D, 9.0-fold (95% CI 8.35–9.64, $P < 0.0001$) for P681H, 46.31-fold (95% CI 42.12–50.49, $P < 0.0001$) for S982A and 8.57-fold (95% CI 7.73–9.42, $P < 0.0001$) for D1118H. However, the T716I variant dramatically decreased entry (0.23-fold [95% CI 0.13–0.34], $P < 0.0001$). The parental B.1.1.7 strain harboring all these mutations showed slightly

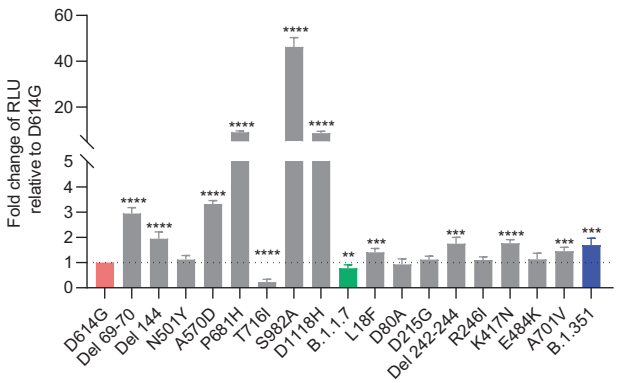

Fig. 2 Mutations in spike altered viral entry of SARS-CoV-2 variants. Two nanograms of pseudotyped virus (based on p24 concentration determined by ELISA) was added to hACE2-expressing 293T cells. Luciferase intensity was measured 2 days later. All experiments were performed in quadruplicate. RLUs of different variants were compared with the results for D614G. Data were analyzed for statistical significance using unpaired Student's *t* test between the reference (D614G) group and other groups. Data are shown as the mean with SD in each group. $^{**}P < 0.01$; $^{***}P < 0.001$; $^{****}P < 0.0001$

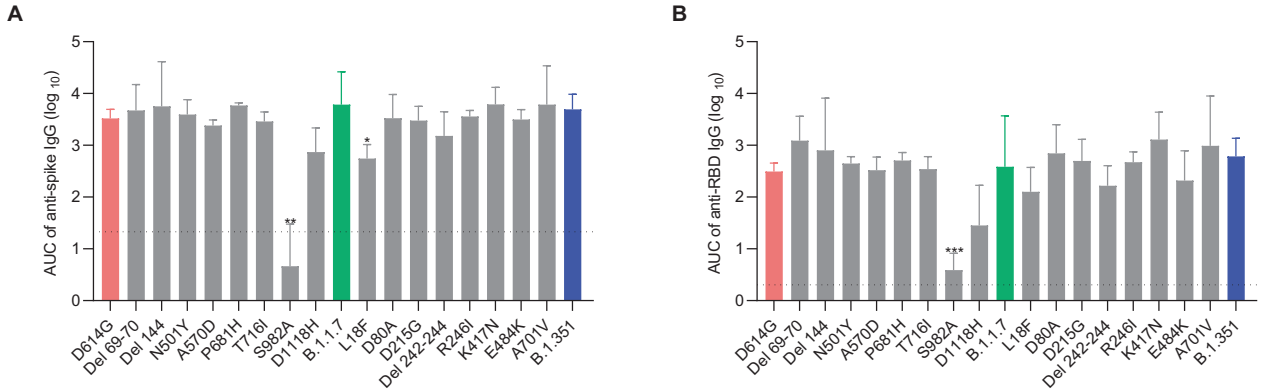

Fig. 3 Substitution of S982A and L18F weakens the generation of binding antibodies. The area under the curve (AUC) of anti-spike (**A**) and anti-RBD (**B**) IgG induced by the 19 designed groups of DNA immunogens ($n = 3$ for each group). The AUC represents the total peak area calculated from ELISA OD values by GraphPad Prism v8. Data were analyzed for statistical significance using the unpaired Student's *t* test. Data are shown as the mean with SD in each group. Dotted black lines indicate the limit of quantification (LOQ). *$P < 0.05$; **$P < 0.01$; ***$P < 0.001$

decreased infectivity compared to D614G (0.78-fold [95% CI 0.61–0.94], $P = 0.0058$) (Fig. 2). Similarly, variants in B.1.351 also promoted viral entry into HEK293T-ACE2 cells (1.41-fold [95% CI 1.22–1.60, $P = 0.0004$] for L18F; 1.75-fold [95% CI 1.43–2.06, $P = 0.0002$] for Del 242–244; 1.77-fold [95% CI 1.55–2.0, $P < 0.0001$] for K417N; 1.46-fold [95% CI 1.29–1.62, $P = 0.0001$] for A701V). The parental B.1.351 strain displayed 1.70-fold (95% CI 1.38–2.03, $P = 0.003$) higher entry into ACE2 cells. Notably, E484K and N501Y alone did not affect viral entry significantly (Fig. 2). These data indicated that individual spike mutations in B.1.1.7 and B.1.351 might have potential impacts on viral entry. Such potential, however, can also vary due to other compensatory mutations in the viral spike.

S982A significantly reduced the induction of the spike-specific antibody response

The spike glycoprotein contains major antigenic determinants for antibody induction. We sought to determine whether spike mutations or deletions would affect vaccine immunogenicity. For this purpose, groups of 6-week-old male BALB/c mice were immunized with equal amounts of each of 19 different DNA vaccines bearing naturally occurring mutants or deletions as mentioned above. After standard 2-dose vaccinations, anti-spike and anti-RBD IgG responses were tested by ELISA. We found that anti-spike and anti-RBD IgG were detected in all 19 groups of mice, demonstrating that all mutants were immunogenic. However, two substitutions of S982A and L18F showed significantly low levels of anti-spike IgG (0.66 [95% CI 1.35–2.68] for S982A and 2.74 [95% CI 2.07–3.42] for L18F vs. 3.52 [95% CI 3.09–3.95] for D614G, $P = 0.004$, $P = 0.0139$) (Fig. 3A). S982A also induced significantly lower levels of anti-RBD IgG than the D614G mutant (0.59 [95% CI −0.21–1.39] vs. (2.49 [95% CI 2.09–2.89], $P = 0.0008$) (Fig. 3B). Considering that coating the Wuhan-Hu-1 spike antigen in ELISA plates might affect the detection of binding antibodies to variants, flow cytometry was used to determine the binding of immunized sera with the corresponding mutant-containing spike-transfected 293T cells. The fluorescence intensity in S982A subjects was consistently weaker than that in other groups (Fig. S2). In contrast, the parental B.1.1.7 strain containing S982A did not show reduced immunogenicity. These results demonstrated that the single S982A substitution substantially reduced DNA vaccine immunogenicity while greatly enhancing viral entry as described above.

Cross-neutralizing antibodies elicited by mutants against major circulating VOCs

Since neutralizing antibodies (NAbs) were reported to be critical for protection [31], cross-NAbs induced by different DNA vaccines were tested against available major VOCs. Compared to D614G, immunized sera of A570D, P681H, S982A, L18F, D215G, Del 242–244 and E484K showed reduced NAbs to at least one variant (Fig. 4A, B). Immunized sera of S982A and L18F showed the lowest NAbs against nearly all circulated VOCs, in accordance with their poor ability to elicit binding antibodies (Fig. 4A, B). In contrast, immunized sera of Del 69–70, Del144, R246I, K417N and A701V displayed enhanced or comparable cross-NAbs against VOCs compared with D614G (Fig. 4A, B). Notably, E484K and A701V elicited stronger NAbs against B.1.351. Furthermore, B.1.351 induced broader NAbs, especially against B.1.351 and B.1.617.2, but no significant differences were observed against the WT virus (Fig. 4A, B). In addition, nearly all the immunogens showed reduced titers of NAbs against B.1.351 and B.1.1.529 (Fig. S3). The majority of immunized mice showed undetectable NAbs against B.1.1.529 (Fig. S3), indicating major immune evasion by B.1.1.529. These data demonstrated that SARS-CoV-2 spike mutations influenced the magnitude of NAb induction. To explore the potential factors responsible for the diversity of immunogenicity induced by the different mutants, quantitative expression of the spike protein was determined by Western blotting. The in vitro results showed lower expression of the S982A spike protein, specifically a reversed ratio of full spike to S1, compared to other mutants (Supplementary Fig. 4A, B), which was speculated to drive the inability of S982A to induce cross-NAbs induction by S982A.

Spike mutations of B.1.1.7 and B.1.351 interfered slightly with T-cell responses

Since cellular immunity also contributes to immune protection, we sought to determine whether spike mutations would affect T-cell responses. Antigen-specific T-cell responses were measured by ICS in response to peptide pools covering the WT spike and peptide pools spanning the mutated regions (Supplementary Table 4). First, the frequencies of WT spike-specific IFN-γ^+CD4$^+$ T cells and IFN-γ^+CD8$^+$ T cells were analyzed. All experimental groups exhibited detectable and nearly comparable levels of T-cell responses relative to D614G (all $P > 0.05$), except for a lower level in the S982A-immunized group (Fig. 5A, B). The overall frequencies of spike-specific IFN-γ^+CD8$^+$ T cells were much higher than those of CD4$^+$ T cells (Fig. 5A, B). Furthermore, the recognition of peptide pools derived from VOCs (peptides covering all spike substitutions in the B.1.1.7 and B.1.351 lineages) and site mutation-containing peptides were also assessed (Supplementary Table 4). IFN-γ^+CD4$^+$ T or CD8$^+$ T cells elicited in response to WT spike peptide pools were detectable in all three mice immunized with D614G, B.1.1.7, and B.1.351 (Fig. 5C, D). Two out of three (2/3) mice (D614G and B.1.1.7) and 3/3 (B.1.351) immunized mice

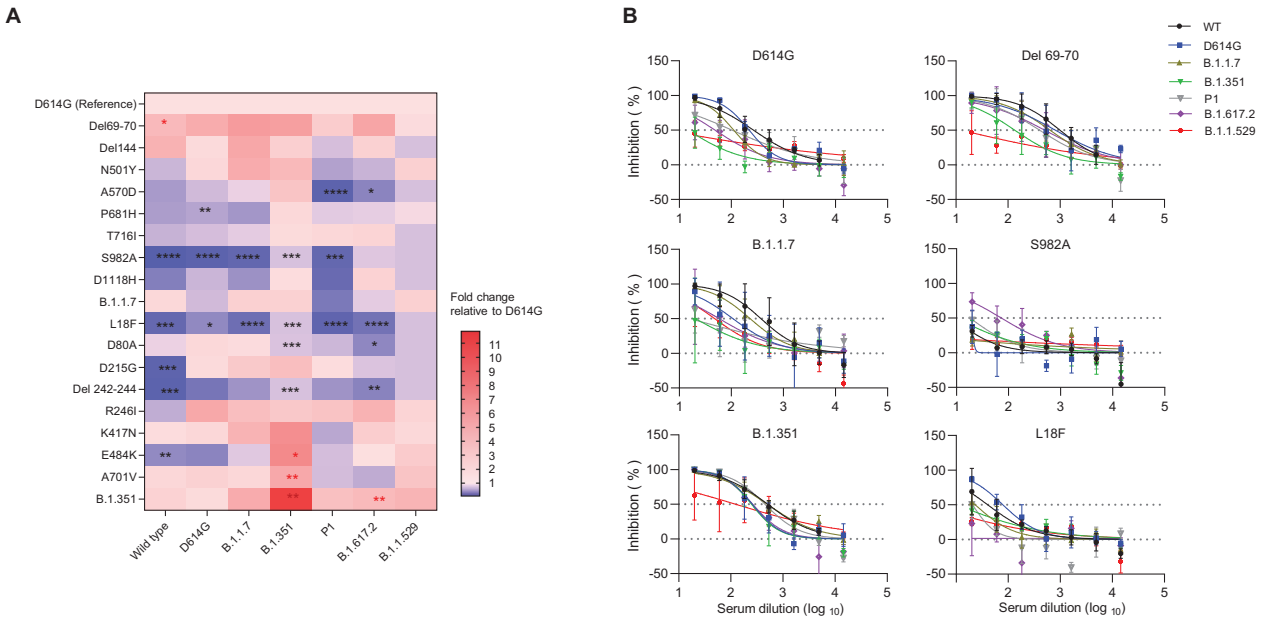

Fig. 4 Cross-neutralizing antibodies induced by different mutants against different VOCs. **A** Comparison of the fold changes of neutralizing IC_{50} relative to D614G elicited by 19 groups of DNA immunogens (y-axis) against different VOCs, including the wild type, D614G, B.1.1.7, B.1.351, P1, B.1.617.2 and B.1.1.529 (x-axis). **B** Typical percent inhibition of D614G-, B.1.1.7-, B.1.351-, Del 69–70-, S982A-, and L18F-immunized sera against major VOCs, including the wild-type (Wuhan-Hu-1), D614G, B.1.1.7, B.1.351, P1, B.1.617.2 and B.1.1.529. Data were analyzed for statistical significance using the unpaired Student's *t* test between the reference (D614G) group and other groups against each VOC. **P* < 0.05; ***P* < 0.01; ****P* < 0.001; *****P* < 0.0001

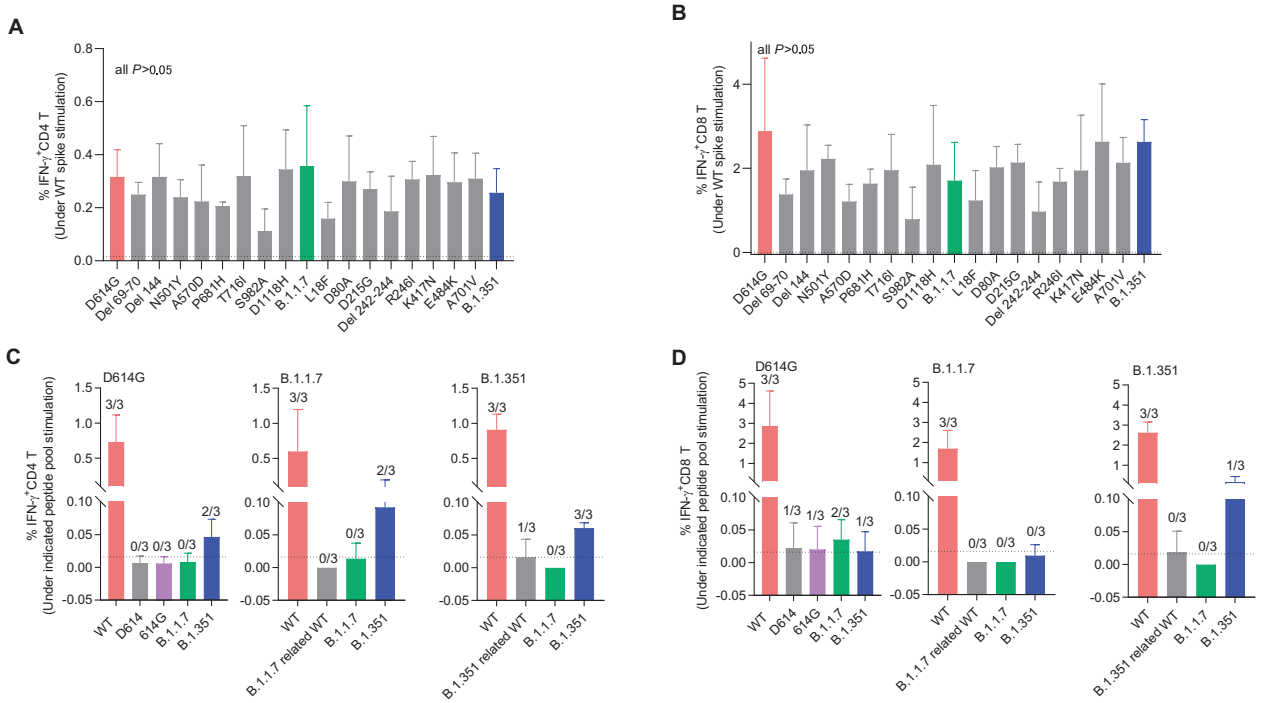

Fig. 5 Mutations in the spike proteins of B.1.1.7 and B.1.351 slightly interfere with the T-cell responses to SARS-CoV-2. The frequencies of spike-specific IFN-γ^+CD4$^+$ T cells (**A**) and IFN-γ^+CD8$^+$ T cells (**B**) elicited by 19 groups of DNA immunogens after stimulation with the full wild-type spike peptide pool (Wuhan Hu-1). Data were analyzed for statistical significance using an unpaired Student's *t* test. Data are shown as the mean with SD in each group. The percentage of antigen-specific IFN-γ^+CD4$^+$ T cells (**C**) and IFN-γ^+ CD8$^+$ T cells (**D**) induced by the D614G, B.1.1.7 and B.1.351 lineages to different ex vivo antigen peptide mixture stimulations, including the full wild-type spike peptide pool (WT), wild-type amino acid-containing peptide pool, mutation-containing peptide pool, B.1.1.7 pool (Alpha) and B.1.351 pool (Beta) (detailed peptide pool information is provided in Supplementary Table 4). The numbers above each bar indicate the numbers of positive responders. Dotted black lines indicate the limit of quantification (LOQ) in (**A**–**D**)

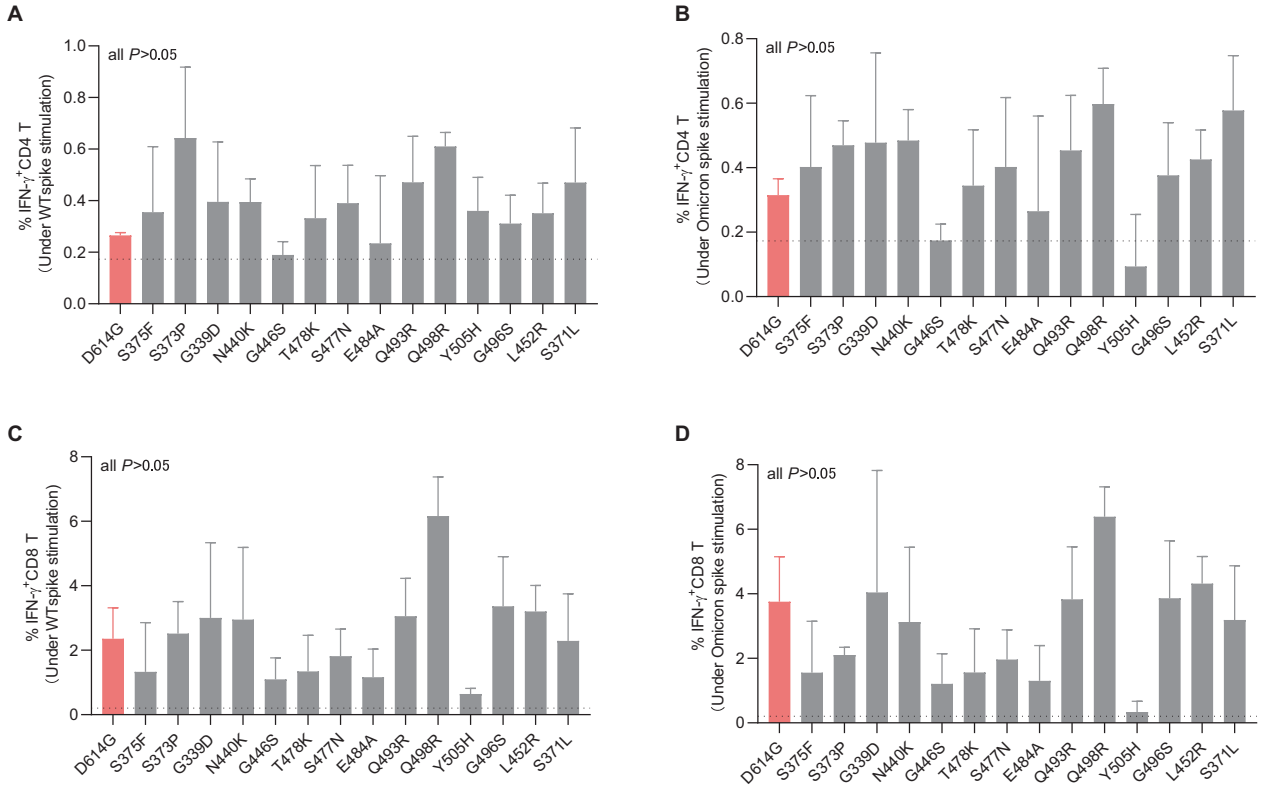

Fig. 6 T-cell response to a single spike mutation of B.1.1.529. The frequencies of spike-specific IFN-γ$^+$CD4$^+$ T cells (**A**, **B**) and IFN-γ$^+$CD8$^+$ T cells (**C**, **D**) elicited by 14 groups of DNA immunogens covering the RBD domain of B.1.1.529 mutants after stimulation with the full wild-type spike peptide pool (Wuhan Hu-1) and the B.1.1.529 spike peptide pool. Data were analyzed for statistical significance using the unpaired Student's *t* test. Data are shown as the mean with SD in each group. Dotted black lines indicate the limit of quantification (LOQ) in (**A**–**D**)

showed a detectable CD4$^+$ T-cell response, yet 1/3 mice (D614G and B.1.351) had a measurable CD8$^+$ T-cell response in recognition of the B.1.351 peptide pool (Fig. 5C, D). Moreover, 2/3 and 1/3 mice immunized with D614G displayed weak but detectable CD8+ T cells in response to the B.1.1.7 and D614 or 614G peptide pools (Fig. 5D). When looking into the impact of individual mutations, all immunized mice displayed detectable amounts of WT spike-specific IFN-γ$^+$CD4$^+$ T- or CD8$^+$ T-cell responses (Fig. S5, S6). Except for L18F and D215G, other immunogens elicited some degrees of IFN-γ$^+$CD4$^+$ T-cell responses to the B.1.351 peptide pool (Fig. S5). Mutations located at residues 144, 501, 681, 80, 246, 242–244, and 701 might affect epitopes contributing to the antigen-specific IFN-γ$^+$CD4$^+$ T-cell response (Fig. S5). Conversely, only Del 69–70-, N501Y-, P681H- and L18F-immunized mice showed measurable IFN-γ$^+$CD8$^+$ T cells in response to B.1.351, whereas Del 144-, S982A-, R246I-, and E484K-immunized mice showed responses to B.1.1.7. Similarly, Del69–70, Del 144, N501Y and T716I might affect epitopes for antigen-specific IFN-γ$^+$CD8$^+$ T-cell responses (Fig. S6). These data suggested that most mutations in the spike proteins of B.1.1.7 and B.1.351 may not influence the induction of T-cell responses significantly. Epitope-containing spike mutations of B.1.1.7 and B.1.351 were not dominant in inducing T-cell responses, although some mutations in B.1.351 made minor contributions to the total spike-specific T-cell responses.

T-cell response to a single spike mutation of B.1.1.529

SARS-CoV-2 B.1.1.529 has extremely rapid spread and has replaced Delta VOC since the end of November 2021 [32]. Here, we determined the T-cell responses to a single spike mutation from the RBD domain of B.1.1.529 in mice (Supplementary Table 4). Consistently, the majority of single B.1.1.529 RBD mutations could induce a stronger CD8 T-cell response (Fig. 6C, D) than CD4 T-cell response (Fig. 6A, B), and the response comparably recognized both WT and B.1.1.529 spike peptide pools (all $P > 0.05$). However, G446S and Y505H mutations showed relatively weaker T-cell responses than D614G and other single B.1.1.529 RBD mutations (Fig. 6A–D). In addition, we found that all 14 single B.1.1.529 RBD mutant-immunized mice could not recognize the peptide pools that only contained the mutation sites except for low frequencies of the IFN-γ$^+$CD8$^+$ T-cell response in Q493R-immunized mice by variant peptides (Fig. S7), indicating that the mutations on the RBD domain of the B.1.1.529 variant were not the epitope for the induction of T-cell responses.

DISCUSSION

Here, we report the biological impact of naturally occurring spike mutations on viral infectivity and vaccine immunogenicity, including cross-reactive immune responses against current major VOCs. Our findings indicated that some spike mutations facilitate the entry of SARS-CoV-2, likely contributing to enhanced viral transmissibility. We also demonstrated that different spike mutations result in distinct humoral immune responses in the context of DNA vaccination in mice with either strengthened or weakened cross-neutralizing activities against VOCs. Moreover, the magnitude of elicited T-cell immunity was influenced slightly by the spike mutations tested. Our results have implications for SARS-CoV-2 vaccine design and optimization against emerging VOCs.

SARS-CoV-2 variants have been circulating for more than 2 years. Several VOCs, including D614G, B.1.1.7 (Alpha), B.1.351 (Beta), P1 (Gamma), B.1.617.2 (Delta) and B.1.1.529, emerged over time, with Omicron currently being the dominant VOC [33]. Unfortunately, the speed of VOC emergence is somewhat faster than our in vivo characterization of the effects of individual spike mutations on vaccine immunogenicity. In this study, we

determined the impact of naturally occurring spike mutations in the Alpha and Beta lineages on viral entry and vaccine immunogenicity. Our results indicated that most mutations in these two lineages, such as L18F/Del69–70/Del144/Del242–244 in NTD, K417N in RBD, A570D in SD1, P681H in SD2, and A701V/S982A/D1118H in S2, could significantly increase viral entry into targeted cells, thus improving the fitness of SARS-CoV-2. Conversely, one mutation, T716I in S2, was observed to reduce viral entry. Ultimately, the Alpha lineage appeared to have slightly decreased infectivity, while the Beta variant outcompeted D614G, indicating that naturally occurring spike mutations determined viral infectivity and transmissibility. Consistent with our findings, Del 69–70/P681R were previously reported to be associated with increasing infectivity and transmissibility by others [34, 35]. Recently, the 3-D structural features of the Omicron spike revealed that mutations could promote an active conformation with enhanced stability and attachment to the cellular receptor ACE2 [36]. Interestingly, we found that the single mutation S982A enhances viral entry while reducing NAb induction. Structural analysis of the SARS-CoV-2 spike protein of the B.1.1.7 variant revealed that the S982A substitution increases the presentation of the "up" RBD state by changing the charge or hydrophobicity at this site, repositions the S2 domain after fusion, allowing for heptad repeat domains to interact with the cell membrane, and thus increases the binding ability with ACE2 [37–40]. The underlying mechanism causing the inability to produce cross-Nabs may be linked with the low expression efficiency of the S982A-containing spike as well as the shifted ratio of the whole spike to S1 (Fig. S4). The opposite effect induced by S982A in B.1.1.7, on the other hand, highlights the allosteric effects of variations in S2 on RBD disposition. Substitutions in B.1.1.7 that destabilize the 3-RBD-down or closed state to favor RBD-up or open states are compensated by substitutions that stabilize the prefusion spike conformation, such as T716I versus D1118H and A570D versus S982A [37]. Since this mutation is not directly involved in ACE2 interaction, its impact on both viral entry and vaccine immunogenicity highlights the importance of investigating the dynamic nature of spike conformation.

NAb resistance induced by spike mutations in VOCs has threatened the efficacy of currently available SARS-CoV-2 vaccines, which are expected to be one of the most cost-effective ways to terminate the COVID-19 pandemic. We and others have reported recently that 2-dose vaccine-induced NAbs titers are significantly reduced (e.g., 2–40-fold) against VOCs, particularly against Beta, Delta and Omicron [21, 41, 42]. In this study, we provided experimental evidence that in addition to spike mutation-mediated NAb resistance, individual mutations such as A570D, P681H, S982A, L18F, D215G, Del 242–244 and E484K have weakened the generation of NAbs. Conversely, individual mutations such as Del 69–70, Del 144, R246I, K417N and A701V could rescue the induction of NAbs. The biological impact of various mutations observed in VOCs should also be carefully evaluated in the context of combined mutation composition, which generates real antigenic determinants. In support of this notion, we found that when the B.1.1.7 spike was used for vaccination, potent NAbs comparable to those elicited by the WT were still induced in the presence of S982A.

The Beta B.1.351 spike was likely a good immunogen with the capacity to elicit broad NAbs against both Beta and Delta variants compared with other immunogens tested. In line with this observation, natural B.1.351 infection resulted in robust cross-NAbs against D614G and P1, which was different from natural D614G infection [26]. In a mouse model, primary vaccination with a modified B.1.351 candidate could induce broader and stronger cross-Nabs against VOCs, especially B.1.351 [43, 44]. NAbs induced by B.1.351 displayed stronger neutralizing ability against Omicron than other immunogens tested [21, 41, 42]. Moreover, we recently reported that Omicron natural infection dramatically augmented cross-reactive NAbs, especially to Beta, Delta and itself. In addition, exploratory studies in a mouse model and human clinical trials indicated increased and comparable titers against VOCs regardless of the composition of the booster dose [43, 45]. However, the inferiority of the 4th dose boost of mRNA or inactivated vaccine to the 3rd dose in terms of humoral immune response revealed that updated vaccines based on VOCs with more diverse epitopes could be used as boosters for eliciting broader NAbs against VOCs [46, 47]. Therefore, it is necessary to determine the influence of VOC single mutations on immune responses after 2-dose wild-type vaccination in the future, which is of great importance for the development of VOC-targeted vaccines.

T-cell immunity plays an important role in protection against SARS-CoV-2 infection [27]. Few studies have evaluated the influence of spike mutations on eliciting a T-cell immune response against VOCs. For this reason, we measured the magnitude of T-cell responses induced by DNA vaccines carrying spike mutations as immunogens. Comparable spike-specific $CD4^+$ or $CD8^+$ T-cell frequencies were detected in patients infected with the WT and the Beta variant in South Africa [48]. Similarly, comparable spike-specific T-cell responses to WT were observed in Omicron BA.1-infected patients as well as in WT-, Beta- and Delta-infected patients [49]. Using peptides spanning the WT, Alpha and Beta mutated regions, no or very low $CD4^+$ or $CD8^+$ T cells could be detected throughout this study. It is possible that B-cell and T-cell epitopes do not overlap in these peptides tested. Alternatively, individual mutations tested were not located in the immune dominant T-cell epitopes. Notably, Riou et al. identified three T cell epitopes containing the D215, L18 or D80 residues, all of which are related to the Beta variant in humans [48]. Mutations containing Del 69–70 and 144 in Alpha were also reported to predict cross-recognition against VOC [50]. Residues 154–254, 296–370 and 682–925 were identified as immunodominant regions [51]. The cross-recognition against different VOCs in patients or vaccinated individuals strongly indicated that conserved T-cell epitopes remained unaffected by spike mutations [48, 52–57]. In fact, only 7% and 3% of previously recognized CD4 and CD8 T-cell epitopes were reported to be affected by mutations in different VOCs [54]. Taken together, these studies revealed the overall preservation of T-cell epitopes, possibly contributing to vaccine efficacy against hospitalization, severity, and mortality despite substantial loss of NAbs against VOCs. Since only 33% of CD4 and 26% of CD8 dominant epitopes were derived from the spike protein, T-cell-based vaccines may consider other viral proteins as immunogens [51]. Generally, spike mutations likely contribute more to NAb escape than T-cell escape. This study was conducted with a focus on spike mutations in D614G, B.1.1.7, B.1.351 and B.1.1.529 RBDs. Subsequently emerged mutations found in the newest VOCs remain to be determined.

DATA AVAILABILITY

The authors declare that the data supporting the findings of this study are available from the corresponding author upon request.

REFERENCES

1. Polack FP, Thomas SJ, Kitchin N, Absalon J, Gurtman A, Lockhart S, et al. Safety and efficacy of the BNT162b2 mRNA Covid-19 vaccine. N Engl J Med. 2020; 383:2603–15.
2. Voysey M, Clemens SAC, Madhi SA, Weckx LY, Folegatti PM, Aley PK, et al. Safety and efficacy of the ChAdOx1 nCoV-19 vaccine (AZD1222) against SARS-CoV-2: an interim analysis of four randomised controlled trials in Brazil, South Africa, and the UK. Lancet. 2021;397:99–111.
3. Sadoff J, Gray G, Vandebosch A, Cárdenas V, Shukarev G, Grinsztejn B, et al. Safety and efficacy of single-dose Ad26. COV2. S vaccine against Covid-19. N Engl J Med. 2021;384:2187–201.
4. Palacios R, Batista AP, Albuquerque CSN, Patiño EG, Santos JDP, Tilli Reis Pessoa Conde M, et al. Efficacy and safety of a COVID-19 inactivated vaccine in

healthcare professionals in Brazil: the PROFISCOV study. SSRN. 2021; https://doi.org/10.2139/ssrn.3822780.
5. Al Kaabi N, Zhang Y, Xia S, Yang Y, Al Qahtani MM, Abdulrazzaq N, et al. Effect of 2 inactivated SARS-CoV-2 vaccines on symptomatic COVID-19 infection in adults: a randomized clinical trial. JAMA. 2021.
6. Kow CS, Hasan SS. Real-world effectiveness of BNT162b2 mRNA vaccine: a meta-analysis of large observational studies. Inflammopharmacology. 2021;29:1075–90.
7. Li X-N, Huang Y, Wang W, Jing Q-L, Zhang C-H, Qin P-Z, et al. Effectiveness of inactivated SARS-CoV-2 vaccines against the Delta variant infection in Guangzhou: a test-negative case–control real-world study. Emerg Microbes Infect. 2021;10:1751–9.
8. Corchado-Garcia J, Zemmour D, Hughes T, Cristea-Platon T, Lenehan P, Pawlowski C, Bade S, et al. Analysis of the Effectiveness of the Ad26.COV2.S Adenoviral Vector Vaccine for Preventing COVID-19. JAMA Netw Open. 2021;4:e2132540.
9. Yurkovetskiy L, Wang X, Pascal KE, Tomkins-Tinch C, Nyalile TP, Wang Y, et al. Structural and functional analysis of the D614G SARS-CoV-2 spike protein variant. Cell. 2020;183:739–51.e8.
10. Benton DJ, Wrobel AG, Xu P, Roustan C, Martin SR, Rosenthal PB, et al. Receptor binding and priming of the spike protein of SARS-CoV-2 for membrane fusion. Nature. 2020;588:327–30.
11. Zhu X, Mannar D, Srivastava SS, Berezuk AM, Demers J-P, Saville JW, et al. Cryo-electron microscopy structures of the N501Y SARS-CoV-2 spike protein in complex with ACE2 and 2 potent neutralizing antibodies. PLoS Biol. 2021;19:e3001237.
12. Deng X, Garcia-Knight MA, Khalid MM, Servellita V, Wang C, Morris MK, et al. Transmission, infectivity, and neutralization of a spike L452R SARS-CoV-2 variant. Cell. 2021;184:3426–37.
13. Thomson EC, Rosen LE, Shepherd JG, Spreafico R, da Silva Filipe A, Wojcechowskyj JA, et al. Circulating SARS-CoV-2 spike N439K variants maintain fitness while evading antibody-mediated immunity. Cell. 2021;184:1171–87.e20.
14. Starr TN, Greaney AJ, Hilton SK, Ellis D, Crawford KH, Dingens AS, et al. Deep mutational scanning of SARS-CoV-2 receptor binding domain reveals constraints on folding and ACE2 binding. Cell. 2020;182:1295–310.e20.
15. Kemp SA, Collier DA, Datir RP, Ferreira IA, Gayed S, Jahun A, et al. SARS-CoV-2 evolution during treatment of chronic infection. Nature. 2021;592:277–82.
16. Wang P, Nair MS, Liu L, Iketani S, Luo Y, Guo Y, et al. Antibody resistance of SARS-CoV-2 variants B. 1.351 and B. 1.1. 7. Nature. 2021;593:130–5.
17. Tao K, Tzou PL, Nouhin J, Gupta RK, de Oliveira T, Kosakovsky Pond SL, et al. The biological and clinical significance of emerging SARS-CoV-2 variants. Nat Rev Genet. 2021;22:1–17.
18. Wang P, Casner RG, Nair MS, Wang M, Yu J, Cerutti G, et al. Increased resistance of SARS-CoV-2 variant P. 1 to antibody neutralization. Cell Host Microbe. 2021;29:747–51.e4.
19. Mlcochova P, Kemp SA, Dhar MS, Papa G, Meng B, Ferreira IA, et al. SARS-CoV-2 B.1.617.2 Delta variant replication and immune evasion. Nature. 2021;599:114–9.
20. Planas D, Veyer D, Baidaliuk A, Staropoli I, Guivel-Benhassine F, Rajah MM, et al. Reduced sensitivity of SARS-CoV-2 variant Delta to antibody neutralization. Nature. 2021;596:276–80.
21. Peng Q, Zhou R, Wang Y, Zhao M, Liu N, Li S, et al. Waning immune responses against SARS-CoV-2 variants of concern among vaccinees in Hong Kong. EBioMedicine. 2022;77:103904.
22. Hacisuleyman E, Hale C, Saito Y, Blachere NE, Bergh M, Conlon EG, et al. Vaccine breakthrough infections with SARS-CoV-2 variants. N Engl J Med. 2021;384:2212–8.
23. Tang P, Hasan MR, Chemaitelly H, Yassine HM, Benslimane FM, Al Khatib HA, et al. BNT162b2 and mRNA-1273 COVID-19 vaccine effectiveness against the SARS-CoV-2 Delta variant in Qatar. Nat Med. 2021:27:2136–43.
24. Keehner J, Horton LE, Binkin NJ, Laurent LC, Pride D, Longhurst CA, et al. Resurgence of SARS-CoV-2 infection in a highly vaccinated health system workforce. N Engl J Med. 2021;385:1330–2.
25. Kuhlmann C, Mayer CK, Claassen M, Maponga T, Burgers WA, Keeton R, et al. Breakthrough infections with SARS-CoV-2 omicron despite mRNA vaccine booster dose. Lancet. 2022;399:625–6.
26. Moyo-Gwete T, Madzivhandila M, Makhado Z, Ayres F, Mhlanga D, Oosthuysen B, et al. Cross-reactive neutralizing antibody responses elicited by SARS-CoV-2 501Y. V2 (B. 1.351). N Engl J Med. 2021;384:2161–3.
27. Zhou R, To KK-W, Wong Y-C, Liu L, Zhou B, Li X, et al. Acute SARS-CoV-2 infection impairs dendritic cell and T cell responses. Immunity. 2020;53:864–77.e5.
28. Corbett KS, Flynn B, Foulds KE, Francica JR, Boyoglu-Barnum S, Werner AP, et al. Evaluation of the mRNA-1273 vaccine against SARS-CoV-2 in nonhuman primates. N Engl J Med. 2020;383:1544–55.
29. Liu L, To KK-W, Chan K-H, Wong Y-C, Zhou R, Kwan K-Y, et al. High neutralizing antibody titer in intensive care unit patients with COVID-19. Emerg microbes Infect. 2020;9:1664–70.
30. Liu L, Wei Q, Lin Q, Fang J, Wang H, Kwok H, et al. Anti–spike IgG causes severe acute lung injury by skewing macrophage responses during acute SARS-CoV infection. JCI insight. 2019;4:e123158.
31. Wang Z, Lorenzi JC, Muecksch F, Finkin S, Viant C, Gaebler C, et al. Enhanced SARS-CoV-2 neutralization by dimeric IgA. Sci Transl Med. 2021;13:eabf1555.
32. Zhou R, To KK, Peng Q, Chan JM, Huang H, Yang D, et al. Vaccine-breakthrough infection by the SARS-CoV-2 omicron variant elicits broadly cross-reactive immune responses. Clin Transl Med. 2022;12:e720.
33. Taylor L. Covid-19: Omicron drives weekly record high in global infections. BMJ. 2022;376:o66.
34. Meng B, Kemp SA, Papa G, Datir R, Ferriera IA, Marelli S, et al. Recurrent emergence of SARS-CoV-2 spike deletion H69/V70 and its role in the Alpha variant B.1.1.7. Cell Rep. 2021;35:109292.
35. Saito A, Nasser H, Uriu K, Kosugi Y, Irie T, Shirakawa K, et al. SARS-CoV-2 spike P681R mutation enhances and accelerates viral fusion. BioRvix. 2021; https://doi.org/10.1101/2021.06.17.448820.
36. Cui Z, Liu P, Wang N, Wang L, Fan K, Zhu Q, et al. Structural and functional characterizations of infectivity and immune evasion of SARS-CoV-2 Omicron. Cell. 2022;185:860–71.
37. Gobeil SM-C, Janowska K, McDowell S, Mansouri K, Parks R, Stalls V, et al. Effect of natural mutations of SARS-CoV-2 on spike structure, conformation, and antigenicity. Science. 2021;373:eabi6226.
38. Xia S, Wen Z, Wang L, Lan Q, Jiao F, Tai L, et al. Structure-based evidence for the enhanced transmissibility of the dominant SARS-CoV-2 B. 1.1. 7 variant (Alpha). Cell Discov. 2021;7:1–5.
39. Magazine N, Zhang T, Wu Y, McGee MC, Veggiani G, Huang W. Mutations and evolution of the SARS-CoV-2 spike protein. Viruses. 2022;14:640.
40. Cai Y, Zhang J, Xiao T, Lavine CL, Rawson S, Peng H, et al. Structural basis for enhanced infectivity and immune evasion of SARS-CoV-2 variants. Science. 2021;373:642–8.
41. Wall EC, Wu M, Harvey R, Kelly G, Warchal S, Sawyer C, et al. Neutralising antibody activity against SARS-CoV-2 VOCs B. 1.617. 2 and B. 1.351 by BNT162b2 vaccination. Lancet. 2021;397:2331–3.
42. Lu L, Mok B, Chen L, Chan J, Tsang O, Lam B, et al. Neutralization of Severe Acute Respiratory Syndrome Coronavirus 2 Omicron Variant by Sera From BNT162b2 or CoronaVac Vaccine Recipients. Clin Infect Dis. 2022;75:e822–6.
43. Su D, Li X, He C, Huang X, Chen M, Wang Q, et al. Broad neutralization against SARS-CoV-2 variants induced by a modified B.1.351 protein-based COVID-19 vaccine candidate. bioRxiv. 2021. https://doi.org/10.1101/2021.05.16.444369.
44. Wu K, Choi A, Koch M, Elbashir S, Ma L, Lee D, et al. Variant SARS-CoV-2 mRNA vaccines confer broad neutralization as primary or booster series in mice. Vaccine. 2021;39:7394–400.
45. Choi A, Koch M, Wu K, Chu L, Ma L, Hill A, et al. Safety and immunogenicity of SARS-CoV-2 variant mRNA vaccine boosters in healthy adults: an interim analysis. Nat Med. 2021;27:2025–31.
46. Regev-Yochay G, Gonen T, Gilboa M, Mandelboim M, Indenbaum V, Amit S, et al. Fourth dose COVID mRNA vaccines' immunogenicity & efficacy against omicron VOC. medRxiv. 2022. https://doi.org/10.1101/2022.02.15.22270948.
47. Wang J, Deng C, Liu M, Liu Y, Li L, Huang Z, et al. Four doses of the inactivated SARS-CoV-2 vaccine redistribute humoral immune responses away from the Receptor Binding Domain. medRxiv. 2022. https://doi.org/10.1101/2022.02.19.22271215.
48. Riou C, Keeton R, Moyo-Gwete T, Hermanus T, Kgagudi P, Baguma R, et al. Escape from recognition of SARS-CoV-2 Beta variant spike epitopes but overall preservation of T cell immunity. Sci Translational Med. 2021;14:eabj6824.
49. Keeton R, Tincho MB, Ngomti A, Baguma R, Benede N, Suzuki A, et al. T cell responses to SARS-CoV-2 spike cross-recognize Omicron. Nature. 2022;603:1–5.
50. Altmann DM, Reynolds CJ, Boyton RJ. SARS-CoV-2 variants: subversion of antibody response and predicted impact on T cell recognition. Cell Rep Med. 2021;2:100286.
51. Grifoni A, Sidney J, Vita R, Peters B, Crotty S, Weiskopf D, et al. SARS-CoV-2 human T cell epitopes: Adaptive immune response against COVID-19. Cell Host Microbe. 2021;29:1076–92.
52. Jordan SC, Shin B-H, Gadsden T-AM, Chu M, Petrosyan A, Le CN, et al. T cell immune responses to SARS-CoV-2 and variants of concern (Alpha and Delta) in infected and vaccinated individuals. Cell Mol Immunol. 2021;18:2554–6.
53. Tarke A, Sidney J, Methot N, Zhang Y, Dan JM, Goodwin B, et al. Negligible impact of SARS-CoV-2 variants on CD4+ and CD8+ T cell reactivity in COVID-19 exposed donors and vaccinees. BioRxiv. 2021. https://doi.org/10.1101/2021.02.27.433180.
54. Tarke A, Sidney J, Methot N, Yu ED, Zhang Y, Dan JM, et al. Impact of SARS-CoV-2 variants on the total CD4+ and CD8+ T cell reactivity in infected or vaccinated individuals. Cell Rep. Med 2021;2:100355.
55. Woldemeskel BA, Garliss CC, Blankson JN. SARS-CoV-2 mRNA vaccines induce broad CD4+ T cell responses that recognize SARS-CoV-2 variants and HCoV-NL63. J Clin Investig. 2021;131:e149335.

56. Liu J, Chandrashekar A, Sellers D, Barrett J, Jacob-Dolan C, Lifton M, et al. Vaccines elicit highly conserved cellular immunity to SARS-CoV-2 Omicron. Nature. 2022;603:493–6.
57. Gao Y, Cai C, Grifoni A, Müller TR, Niessl J, Olofsson A, et al. Ancestral SARS-CoV-2-specific T cells cross-recognize the Omicron variant. Nat Med. 2022;28:472–6.

ACKNOWLEDGEMENTS

This study was supported by the Hong Kong Research Grants Council Collaborative Research Fund (C7156–20GF to ZC and C1134–20GF); the Research Grants Council General Research Fund (GRF17117422); the Hong Kong Health and Medical Research Fund (COVID1903010-Project 4, COVID190123 and 19181012); the Shenzhen Science and Technology Program (JSGG20200225151410198 and JCYJ20210324131610027); HKU Development Fund and LKS Faculty of Medicine Matching Fund to AIDS Institute; the Hong Kong Innovation and Technology Fund; the Hong Kong Health@InnoHK, Innovation and Technology Commission; and a generous donation from the Friends of Hope Education Fund. ZC's team was also partly supported by the Theme-Based Research Scheme (T11–706/18-N and T11-709/21-N). We sincerely thank Dr. David D. Ho and Pengfei Wang for kindly providing the expression plasmids encoding the D614G, B.1.1.7, B.1.351 variants and single mutation-containing mutants and Dr. Linqi Zhang for B.1.617.2.

AUTHOR CONTRIBUTIONS

ZC supervised the collaborative team, conceived and designed the study, and revised the manuscript. QP and RZ designed some experiments and analyzed the data. QP, RZ, NL and HX immunized the mice. QP, NL, MZ, RZ, DY, KA, and HH performed the immune assays, LL and HW provided critical comments, support and materials. QP and RZ analyzed and verified the data reported in the paper. QP drafted the paper. All authors read and approved the final version of the paper.

COMPETING INTERESTS

The authors declare no competing interests.

ADDITIONAL INFORMATION

Supplementary information The online version contains supplementary material available at https://doi.org/10.1038/s41423-022-00924-8.

Correspondence and requests for materials should be addressed to Zhiwei Chen.

Reprints and permission information is available at http://www.nature.com/reprints